

Computational and neurobiological mechanisms underlying cognitive flexibility

David Badre*^{†‡} and Anthony D. Wagner*

*Department of Psychology and Neurosciences Program, Stanford University, Stanford, CA 94305; and [†]Department of Brain and Cognitive Sciences, Massachusetts Institute of Technology, Cambridge, MA 02139-4307

Edited by Edward E. Smith, Columbia University, New York, NY, and approved March 14, 2006 (received for review November 2, 2005)

The ability to switch between multiple tasks is central to flexible behavior. Although switching between tasks is readily accomplished, a well established consequence of task switching (TS) is behavioral slowing. The source of this switch cost and the contribution of cognitive control to its resolution remain highly controversial. Here, we tested whether proactive interference arising from memory places fundamental constraints on flexible performance, and whether prefrontal control processes contribute to overcoming these constraints. Event-related functional MRI indexed neural responses during TS. The contributions of cognitive control and interference were made theoretically explicit in a computational model of task performance. Model estimates of two levels of proactive interference, “conceptual conflict” and “response conflict,” produced distinct preparation-related profiles. Left ventrolateral prefrontal cortical activation paralleled model estimates of conceptual conflict, dissociating from that in left inferior parietal cortex, which paralleled model estimates of response conflict. These computationally informed neural measures specify retrieved conceptual representations as a source of conflict during TS and suggest that left ventrolateral prefrontal cortex resolves this conflict to facilitate flexible performance.

cognitive control | executive function | memory | prefrontal cortex | task switching

The course of modern life is often interrupted by demands that do not await our disposition but must be addressed immediately. The ability to reconfigure our cognitive system to meet shifting task demands is evident and remarkable. A fundamental problem in the study of cognitive control is specification of the psychological and neural processes by which we achieve this flexibility and successfully switch tasks. Task switching (TS) is studied by comparing episodes in which subjects switch between two simple tasks to those in which they repeat the same task (1–5). In such comparisons, TS incurs slowing in response time (RT), termed a switch cost. As a window onto the mechanisms of flexible performance, considerable attention has focused on characterizing the source of the switch cost, although extant data have generated controversy rather than resolution (2, 4).

Two classes of theory have framed the debate over TS costs. Reconfiguration theories posit time-consuming intentional control processes that initiate reconfiguration of the task set independent of the presentation of a target stimulus (6). From this perspective, the switch cost reflects the time consumed by these control processes, and their progress during a preparation interval yields preparation-related reductions in the switch cost. Alternatively, interference theories propose that switch costs are substantially or wholly attributable to conflict arising from memory due to the recent performance of a different task (2, 7, 8). From one such perspective, performance of a given task primes associations among available cues and task representations (2, 9, 10). Subsequent encounter with these cues in the context of a new task results in facilitated retrieval of the primed but irrelevant information. This proactive interference compromises retrieval of relevant information.

Consideration of the relation between TS and the neural mechanisms of retrieval and interference resolution in memory may bear on these theories, because a central component of both the reconfiguration and interference accounts is the activation of a task set from memory (2, 3, 9, 11). Outside the context of TS, ventrolateral prefrontal cortex (VLPFC) has been associated with the retrieval and selection of task-relevant representations (12–15). In particular, left mid-VLPFC (\approx BA 45; inferior frontal gyrus *pars triangularis*) has been associated with resolution of proactive interference (15, 16) and with overcoming interference during semantic and episodic retrieval (13, 14, 17). Within the context of TS, simple comparisons of switch vs. repeat conditions have revealed a frontoparietal network including VLPFC, in addition to supplementary motor area (SMA) and inferior/superior parietal cortices (18–25).[§] Importantly, the switch-related activation in VLPFC has been modulated in experiments that test both reconfiguration and interference theories of TS (20, 26, 27). We posit that these initial findings, although potentially contradictory, when considered in the context of the broader literature on left VLPFC function, motivate the hypothesis that VLPFC is engaged to overcome interference between competing mnemonic representations retrieved during TS.

Here, we sought to test this hypothesis directly. To provide an explicit theoretical context, a computational model, termed control of associative memory during TS (CAM-TS), was evaluated based on behavioral data (Experiment 1). Indices of two forms of proactive interference, among concepts and responses, were derived from the model, providing quantitative predictions for functional MRI (fMRI) measures (Experiment 2). In Experiment 2, we used fMRI to assess the changes in neural switch effects due to preparation time. Anticipating the results, this manipulation dissociated the pattern of activation in mid-VLPFC from other switch-related regions and related this activation directly to the quantitative predictions of conceptual conflict from CAM-TS.

Results

Experiment 1: Preparation Effects on Behavioral Switch Costs. Experiment 1 characterized the change in RT switch cost due to preparation time, independent of transient decay effects (7, 28), thus providing data on which to evaluate CAM-TS (Fig. 1A). On each trial, subjects were cued as to which task (vowel/consonant or odd/even judgment) was to be performed with the next required target (a letter/digit pair). Half of the trials required a TS, and half required a repeat. Preparedness was manipulated by varying the

Conflict of interest statement: No conflicts declared.

This paper was submitted directly (Track II) to the PNAS office.

Abbreviations: VLPFC, ventrolateral prefrontal cortex; SMA, supplementary motor area; fMRI, functional MRI; RT, response time; TS, task switch/switching; CAM-TS, control of associative memory during TS; CSI, cue-to-stimulus interval; RCI, time from the previous response until cue presentation; RR, response repetition; RS, response same; RD, response different; ROI, region of interest.

[†]To whom correspondence should be addressed at: Helen Wills Neuroscience Institute, 132 Barker Hall, Mail Code 3120, Berkeley, CA 94720-3120. E-mail: dbadre@berkeley.edu.

[§]Meyer, D. E., Lauber, E. J., Rubinsten, J., Gmeindl, L., Junck, L. & Koeppel, R. A., Poster Presented at the Annual Meeting of the Cognitive Neuroscience Society, April 5-7, 1998, San Francisco.

© 2006 by The National Academy of Sciences of the USA

presentation (e.g., ref. 31). Critically, we conceptualize this control process as directly analogous to that proposed for selection from among retrieved competitors during memory retrieval tasks and under short-term proactive interference (13–16) (see supporting information for analysis).

Simulated behavior and conflict estimates. Simulated TS effects from CAM-TS provided a strong fit to the behavioral results from Experiment 1 (Fig. 2*B* and *C*), with the simulated CSI-dependent decline in the RT switch cost closely paralleling the empirically derived decline ($R = 0.96$) and also the impact of RS-enhanced proactive interference across CSI (R values > 0.97). Enhanced conflict due to RR occurs because the irrelevant associations formed on the previous trial are strongest for the previously executed response pathway. In other words, the response itself is a highly effective cue for the irrelevant task set.

Critically, although switching tasks may be accomplished without up-regulation of control, there is no CSI-dependent decline in simulated switch costs when up-regulation is absent (Fig. 2*B*; model fit, $R = 0.49$).

As a source of interference, conflict emerges in CAM-TS due to activation being spread over more competing units in a layer. A quantifiable index of this conflict was computed as Hopfield energy (32, 33) (Fig. 2*A*). The computational properties of Hopfield energy correspond to features of conflict (34), in that energy increases exponentially with the numbers of units over which activation is spread and with the strength of their mutually competitive activation levels. Energy is distinct from the overall level of activation, however, because energy would be highest when multiple nodes are equally active (i.e., competing) but relatively low when only one node is highly active (i.e., not competing).

Strikingly, in CAM-TS, switch-derived conflict in the concept layer during a TS declines across CSI (Fig. 2*A*). By contrast, the response layer shows a generally increasing conflict function with increasing CSI (Fig. 2*A*). Further priming of the irrelevant pathway due to RR also increases conflict values, but in this case, this conflict increase is observed in both the conceptual and response layers.

These patterns emerge from the dynamics of CAM-TS. As noted above, given bias and enough preparation time, the relevant concept units come to dominate the concept layer before target presentation. When only relevant representations dominate, there is less conflict, hence a lower conflict signal at longer CSIs. By contrast, the more the two relevant conceptual representations come to dominate, the more activation feeds forward to the response layer and equates activation among these nodes before the presentation of the target. Hence, conflict may get transiently higher within the response layer with greater preparation before a switch in the concept layer (although enhanced response conflict at a long CSI never reaches the value of conflict in the concept layer at a short CSI). These simulated levels of conflict provide quantitative predictions to guide fMRI analysis.

Experiment 2: VLPFC and Interference Resolution During TS. An independent sample underwent fMRI while performing an adapted version of the Experiment 1 paradigm (Fig. 1*B*). Again, a CSI manipulation varied preparation time (250–1,150 ms), and RR further varied interference. As in Experiment 1, TS incurred a RT switch cost [$F(1,9) = 82.8, P < 0.0001$; Fig. 3]. This cost declined linearly with increasing CSI [$t(9) = 2.4, P < 0.05$], and a residual cost (105 ms) was evident after a 1,150-ms CSI [$F(1,9) = 31.4, P < 0.0001$]. **Effects of preparation time.** According to CAM-TS, conflict in the conceptual layer is maximal at the shortest CSI. Switch vs. repeat differences at the 250-ms CSI were reliable in left mid-VLPFC (\approx BA 45; -51 27 6), left posterior VLPFC (\approx BA 44/6/9; -45 6 27), left dorsolateral prefrontal cortex (\approx BA 46; -36 24 30) and along the superior bank of the intraparietal sulcus bilaterally, inclusive of superior parietal cortex (\approx BA 7/40; -36 -54 51; 30, -54 39; Fig. 4*A*).

Importantly, in region of interest (ROI) analyses, the only region to show a CSI-dependent decline in the neural switch

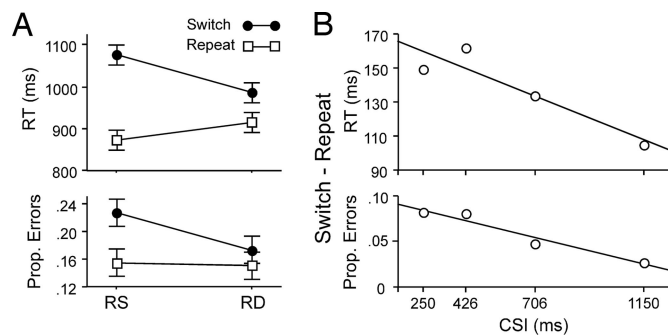


Fig. 3. Plots of RT and error rate from Experiment 2. (A) Depiction of differences between switch and repeat trials as a function of RR (RS vs. RD). (B) The linear decline in RT switch cost across CSI was reliable ($P < 0.05$), and there was a trend for a decline in error rates [$t(9) = 1.9, P = 0.08$].

cost (switch $>$ repeat) was mid-VLPFC [Fig. 4*A*; TS \times CSI: $F(3,27) = 3.8, P < 0.05$]. The magnitude of the neural switch cost was greater at the shortest (250 ms) relative to the longest CSI [1,150 ms; $F(1,9) = 7.8, P < 0.01$]. The pattern of change across CSI was reliably characterized by a monotonic decline [$t(9) = 2.5, P < 0.05$]. In further support of our prediction that this region would be sensitive to the level of interference from retrieved conceptual representations, the neural switch cost in left mid-VLPFC was reliably characterized by the CSI-dependent decline in conflict computed from the concept layer of CAM-TS [$t(9) = 2.7, P < 0.05$; Fig. 4*A*].

Caudal to mid-VLPFC, the posterior VLPFC region showing a neural switch cost, approximates what has been termed the inferior frontal junction (35), a region that, together with mid-VLPFC, has been consistently implicated in TS. However, the magnitude of the neural switch cost in posterior VLPFC across CSI was poorly fit by a monotonically declining function [$t(9) = 0.12, P = 0.9$; Fig. 4*A*], because the switch cost did not differ between the shortest and longest CSIs [$F < 1.0$]. This insensitivity to CSI reliably dissociated posterior VLPFC from mid-VLPFC [$t(9) = 2.6, P < 0.05$].

Voxel-wise analysis of switch vs. repeat trials collapsed across CSI further characterized the neural correlates of TS (Fig. 4*B*). In PFC, greater activation on switch trials was observed in mid-VLPFC/dorsolateral prefrontal cortex (\approx BA 45/46; -54 18 24; -54 33 18; -48 39 18) and posterior VLPFC (\approx BA 44; -45 9 27), as well as in SMA (\approx BA 8; 0 18 48). Neural switch costs were also evident in left inferior (\approx BA 39/40; -33 -63 42; -51 -33 48) and bilateral superior parietal cortex (\approx BA 7; -27 -66 57; 16 -63 60).

Again, the only region to show a CSI-dependent decline in the neural switch cost was the anterior and dorsal extent of mid-VLPFC (-54 33 18; Fig. 4*B*). ROI analysis revealed (i) that the neural switch cost was greater at the shortest relative to the longest CSI [$F(1,9) = 4.0, P = 0.05$], (ii) that the switch cost declined monotonically [$t(9) = 2.7, P < 0.05$], and (iii) that this decrease was reliably characterized by the CAM-TS index of conceptual conflict [$t(9) = 2.8, P < 0.05$].

In contrast to mid-VLPFC, the neural switch cost in inferior parietal cortex (-51 -33 48) tended to increase with longer CSIs, although not reliably [$t(9) < 1.0$]. Qualitatively, this pattern appeared to correspond to the level of conflict arising in the Response layer of CAM-TS, in that both showed a modest ramping response (Fig. 4*B*), although the fit was unreliable when using the standard calculation of conflict [$t(9) = 1.4, P = 0.19$]. However, motivated by the recent hypothesis that inferior parietal neurons may accumulate evidence en route to response selection (36), we recomputed the level of conflict in CAM-TS using accumulated activation in the response layer (for details, see supporting information). This index of accumulated conflict fit the inferior parietal response [$t(9) = 2.9, P < 0.05$; Fig. 4*B*].

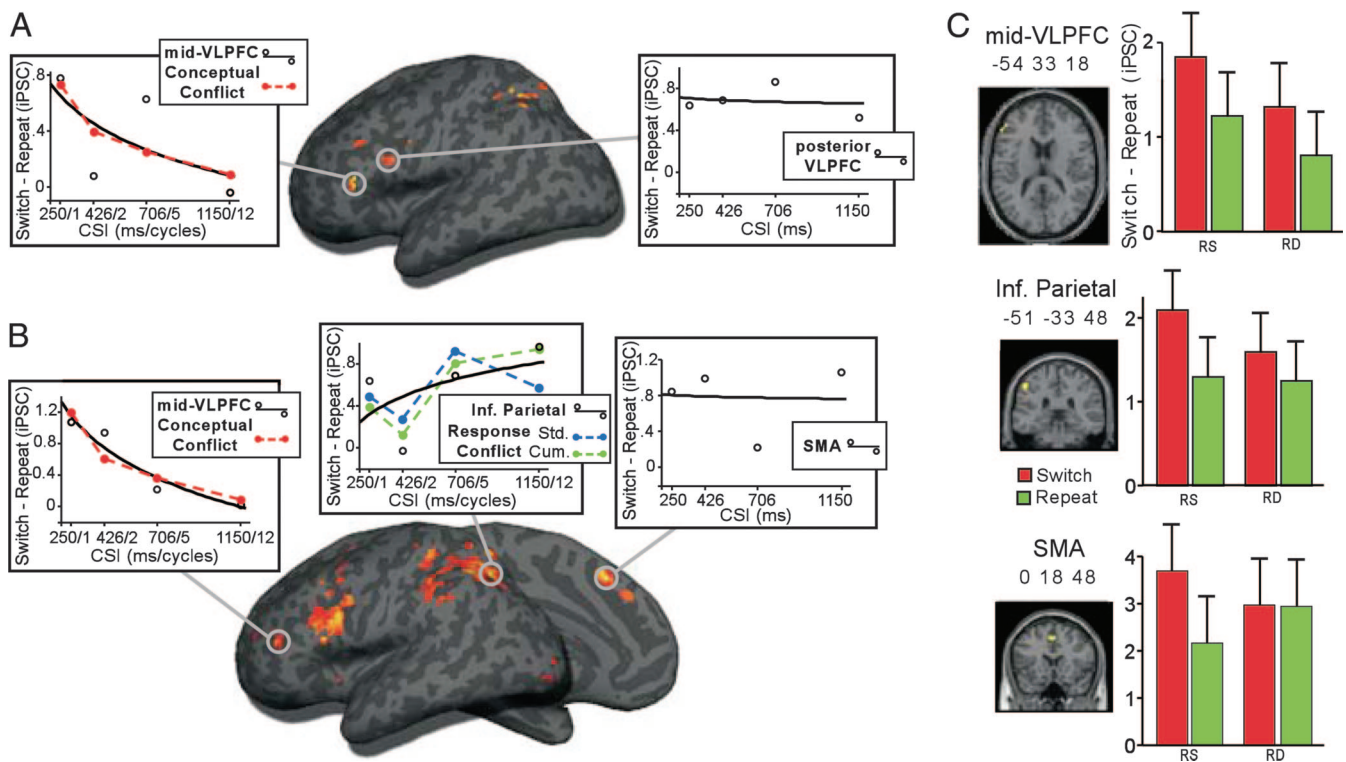


Fig. 4. fMRI results from Experiment 2. (A) Surface rendering of switch > repeat at the shortest CSI (250 ms). Plotted are neural switch costs across CSI from ROI analyses of left mid-VLPFC ($-51\ 27\ 6$) and posterior VLPFC ($-45\ 6\ 27$). (B) The contrast of switch vs. repeat collapsed across CSI. Plotted are changes in neural switch cost from ROIs in left mid-VLPFC ($-54\ 33\ 18$), inferior parietal cortex ($-51\ -33\ 48$), and SMA ($0\ 18\ 48$). Also depicted are linearly scaled conflict signals (dashed lines) from conceptual (red) and response [blue (standard) and green (cumulative)] layers of CAM-TS. (C) Bar graphs depict enhancement of switch costs during RS vs. RD trials split by switch (red bar) and repeat (green bar) from ROIs in left mid-VLPFC ($-54\ 33\ 18$), inferior parietal cortex ($-51\ -33\ 48$), and SMA ($0\ 18\ 48$).

Of central importance, the pattern over CSI in inferior parietal cortex dissociated from the decreasing response in left mid-VLPFC [$t(9) = 3.0$, $P < 0.05$]. Collectively, these data provide strong evidence that mid-VLPFC is recruited in the face of switch-related interference, with CAM-TS suggesting that mid-VLPFC may resolve interference at the conceptual level.

Effects of RR. Proactive interference was also modulated through the manipulation of RR. According to CAM-TS, RR induces increased conflict in multiple layers. Behaviorally, RR enhanced the RT switch cost during fMRI [Fig. 3A; TS \times RR: $F(1,9) = 58.5$, $P < 0.0001$]. Neurally, a TS \times RR interaction was marginally evident in SMA [Fig. 4C; $F(1,9) = 4.3$, $P = 0.06$], reflecting the fact that the effect of TS in SMA was entirely accounted for by RR-induced interference: Switch was greater than Repeat on RS [$F(1,9) = 9.0$, $P < 0.05$] but not RD trials ($F < 1$).

Indicative of RR interference and consistent with the conceptual conflict signal in CAM-TS, planned contrasts also revealed that activation in mid-VLPFC was greater for switch-RS than switch-RD trials [$F(1,9) = 5.2$, $P < 0.05$]. However, in contrast to SMA, neural switch costs on RD trials were also evident in mid-VLPFC (Fig. 4C), activation in mid-VLPFC tended to dissociate from that in SMA, as evidenced by a marginal region [mid-VLPFC/SMA] \times RR \times TS interaction [$F(1,9) = 4.3$, $P = 0.06$]. Finally, qualitatively similar to mid-VLPFC, inferior parietal cortex showed a marginal switch-RS vs. switch-RD difference [$F(1,9) = 4.7$, $P = 0.06$].

Conclusion

TS can be understood as an act of memory. Thus, the behavioral and psychological consequences of TS can be understood in terms of the structures, processes, and failures of memory. This proposition entails that the control processes contributing to TS are indistinguishable from the control processes engaged to overcome interference arising during other acts of memory. Accordingly, the

neural mechanisms supporting interference resolution during memory retrieval, such as those subserved by mid-VLPFC, are central for successfully overcoming interference during a TS.

Our results strongly support these conclusions. In particular, we demonstrate that a simple connectionist model deriving its RT switch cost entirely from experience-dependent changes in its associative structure accounts for switch costs through proactive interference at both the conceptual and response levels and accomplishes preparation-related declines in the switch cost through prospective, endogenous control. Strikingly, the model's signature of declining conflict among activated concepts after preparation was characteristic of activity in left mid-VLPFC and dissociated this region from other regions active during TS. Importantly, this monotonic decline in mid-VLPFC did not simply track changes in RT, because both the form of the decline and the lack of a residual cost in mid-VLPFC differentiate these response profiles. Moreover, inferior parietal cortex was associated with a ramping response over CSI, a pattern qualitatively consistent with the increased conflict in the response layer of CAM-TS at longer CSIs. A role for posterior parietal cortex in processing response alternatives finds additional support in the broader cognitive control literature (37, 38). A temporal shift from mid-VLPFC (conceptual) to inferior parietal (response) cortex may also parallel electroencephalogram evidence that TS is accompanied by an early frontal component (≈ 300 – 500 ms) followed by a subsequent parietal component (≈ 500 – $1,000$ ms) (39–41).

It is important to note that, although the behavioral and neuroimaging results confirm the predictions derived from our memory-based model of TS, this does not preclude the possibility that other models based on different assumptions could make similar quantitative predictions. However, such a model must account for several empirical findings reported here that stand independent of the validity of our specific theoretical framework: (i) the CSI-based decline and the RR effect in mid-VLPFC, (ii) the dissociation of

mid-VLPFC from sustained effects in posterior VLPFC and SMA, and (iii) the dissociation of mid-VLPFC from the ramping function in posterior parietal cortex.

This caveat notwithstanding, the present framework and supporting results are broadly appealing, because they provide a potential theoretical reconciliation to the long-standing debate over the origins of TS costs and the contribution of cognitive control to prospectively switching tasks. CAM-TS is unique from other prominent frameworks (7, 42) in its exclusive reliance on learning-based changes as a source of its switch cost, its locus of conflict in the conceptual and response layers as opposed to the control layer, and the intervention of control in reducing costs. CAM-TS assumes that a considerable portion of switch costs is attributable to proactive interference from retrieved irrelevant information. This is consistent with interference accounts of the switch cost and accounts that minimize the direct contribution of control to the length of the switch cost. However, our data also indicate that prospective engagement of control processes that regulate memory may help resolve interference, contributing to preparation-related declines. In this respect, CAM-TS shares an active and strategic control process with reconfiguration models.

A distinguishing feature of this synthesis is its potentially parsimonious account of the neuropsychological data on TS. Again, control in CAM-TS reduces interference and facilitates retrieval rather than enacts a TS. Consequently, the model predicts that in this explicit cueing variant, TS can proceed without endogenous control, although under such circumstances performance is more vulnerable to interference (Fig. 2*B*). Lesion data indicate that damage inclusive of left mid-VLPFC results in an enhanced switch cost but neither prohibits the ability to switch tasks nor results in perseveration (43). CAM-TS accurately predicts this pattern of enhanced cost but not perseveration after mid-VLPFC insult, a point that may favorably distinguish the present model from a related connectionist framework designed to model asymmetric costs (7) or other elegant mathematical models (42) that suggest minimal control.

Finally, the present work does not preclude the contributions of additional control processes or interference effects during TS. A process of goal setting is likely required in many TS contexts (3) and may be associated with distinct regions of PFC, such as frontal polar cortex (22). Furthermore, the unique effects in SMA and posterior VLPFC, not directly accounted for by CAM-TS, point to the multicomponent nature of TS. By contrast, it is of some interest that the anterior cingulate cortex was not sensitive to conceptual or response-level conflict in this task, although this is not necessarily inconsistent with the broader literature on TS (44) or proactive interference (45). Critically, however, the present computational framework and neuroimaging evidence argue that one critical component for flexible behavior is interference resolution by mid-VLPFC.

Methods

Subjects. Twenty-four right-handed native English speakers (16 female; ages 18–25 yrs) were remunerated \$10 per hour for participation in Experiment 1, and 13 right-handed native English speakers (8 female; ages 18–25 yrs) were remunerated \$50 for participation in Experiment 2. Data from three subjects from Experiment 2 (one female) were excluded before fMRI analysis because of high nonresponse rates due to a difficulty with responding before the response deadline. Informed consent was obtained as approved by the human subjects committees at Massachusetts General Hospital, Massachusetts Institute of Technology, and Stanford University.

Experiment 1: Design and Procedure. Stimuli consisted of number-letter pairs (e.g., “2b”) presented centrally in 32-point Monaco font. Pairs were constructed from a set of 10 letters, five consonants (“p,” “f,” “n,” “k,” “s”), and five vowels (“a,” “e,” “i,” “o,” “u”), and a set of 10 digits, five odd numbers (“1,” “3,” “5,” “7,” “9”), and five

even numbers (“0,” “2,” “4,” “6,” “8”). The number and letter positions were counterbalanced across pairs (e.g., “2b” or “b2”).

Subjects performed one of two categorization tasks (Fig. 1*A*) with each stimulus pair. In the number task, subjects categorized the number as odd or even. In the letter task, subjects categorized the letter as vowel or consonant. Categorization decisions for both tasks were reported by using one of the same two buttons (left or right) under the right hand.

During each block of the experiment, the number and letter tasks were intermixed. An instruction cue (LETTER or NUMBER) preceded the onset of each target stimulus (Fig. 1) and signaled the task to be performed for that target. The trial terminated once a response was made. The correct response could be the same as (RS) or different from (RD) the response emitted on the previous trial. The RCI varied among four values (50, 226, 506, or 950 ms) that expanded logarithmically. Likewise, the CSI varied among four values (50, 226, 506, or 950 ms, plus 200 ms for cue presentation). To maximize our ability to detect switch-related declines (6), CSI was blocked, and the order of blocks was fully counterbalanced between subjects.

After four excluded warm-up trials, each CSI-defined block consisted of 256 trials divided evenly among remaining experimental conditions. In addition, trials were counterbalanced for (i) the match of the irrelevant flanker response to the correct response, and (ii) whether the correct target position switched from the previous trial.

All behavioral testing was conducted on a Macintosh G4 computer in a darkened testing room at Stanford University. Before data collection, subjects received extensive training. Subjects continuously practiced one of the tasks (e.g., letter or number) alone and then practiced the other task (e.g., number or letter). Then subjects practiced switching between the tasks in four short blocks at each CSI in experimental order.

Experiment 2: Design and Behavioral Procedures. Stimuli for the fMRI experiment were identical to those used in Experiment 1. As in Experiment 1, subjects performed either the number or letter task (Fig. 1*B*), although making responses with their left hand. Before fMRI data collection, subjects received extensive training: (i) outside the scanner, subjects continuously performed the letter task and then the number task, and (ii) subsequently, subjects practiced switching between the tasks.

During fMRI scanning, the number and letter tasks were intermixed. An instruction cue preceded the onset of each stimulus (Fig. 1*B*) and signaled the upcoming task. During the CSI within a trial and the intertrial interval (ITI) separating trials, a white fixation cross was presented centrally (as a preparatory warning, the fixation cross turned from white to red immediately before cue/stimulus presentation). To allow for estimation and deconvolution of the hemodynamic response as a function of small changes in CSI duration, trials were grouped into pairs of two task events (T-1 and T-2), although to the subject, the experiment appeared as a continuous stream of task events. The onset of the first task event (T-1) in each pair followed a variable-duration null fixation period (2–16 s) that followed the prior pair. To permit event-related fMRI analyses, T-1 always required performance of the same task that had just been performed (task repeat) during the T-2 phase of the prior pair. Furthermore, the consonance of the T-1 manual response to the manual response emitted during the T-2 phase of the prior pair (RD/RS) and the target and flanker relationship within T-1 were counterbalanced across experimental conditions at T-2. The CSI duration for T-1 was fixed at 1,000 ms, and the ITI between T-1 and the T-2 cue was always 50 ms.

The critical experimental variables were manipulated during T-2. The task for T-2 was either a repeat or switch from that during T-1. The T-2 manual response (left or right) was either the same as (RS) or different from (RD) that required during T-1. Finally, the duration of the CSI (inclusive of 200-ms task cue) for the T-2 event

varied (250 s; 426, 706, or 1,150 ms). Target position was also counterbalanced across T-1/T-2 pairs. Collectively, this design allowed for analysis of fMRI signal differences at T-2 according to the critical factor manipulations (repeat vs. switch, RS vs. RD, and CSI duration). For all events, a response deadline of 1,800 ms was imposed. For the imaging analysis, a pair was considered incorrect if a subject responded incorrectly or failed to respond before the response deadline on T-1 and/or T-2 within the pair. Analysis of RT was restricted to the trials included in the imaging analysis; error analysis was based only on T-2 events and did not depend on T-1 accuracy.

During fMRI scanning, subjects encountered 480 pairs of trials across four scan epochs. Events were grouped into blocks of 30 pairs on the basis of T-2 CSI duration. Subjects encountered a block of each CSI duration during each scan epoch. Response mappings and condition order were counterbalanced across subjects.

fMRI Acquisition and Analysis Procedures. Whole-brain imaging was performed on a 3-T Siemens (Iselin, NJ) Trio MRI system. Functional data were acquired by using a gradient-echo echo-planar pulse sequence [repetition time (TR) = 2 s, echo time (TE) = 30 ms, 21 axial slices, $3.125 \times 3.125 \times 5$ mm, 1-mm interslice gap, four runs \times 756 volume acquisitions]. High-resolution T1-weighted [magnetization prepared rapid gradient echo (MP-RAGE)] structural images were collected for anatomical visualization, during which subjects practiced the tasks. Head motion was restricted by using firm padding surrounding the head. Projected visual stimuli were viewed through a mirror attached to the standard head coil.

Data were preprocessed by using SPM99 (Wellcome Department of Cognitive Neurology, London). Functional images were corrected for differences in slice acquisition timing, followed by motion correction (using sinc interpolation). Structural and functional data were spatially normalized to a template based on the Montreal Neurological Institute stereotaxic space (46) using a 12-parameter affine transformation along with a nonlinear transformation using cosine basis functions. Images were resampled to 3-mm cubic voxels and spatially smoothed with an 8-mm full-width-at-half-maximum isotropic Gaussian kernel.

Statistical models were constructed by using SPM99 under the assumptions of the general linear model. The units of analysis were the task pairs described above (Fig. 1B). Because the T-1 phase of each pair was counterbalanced across the T-2 conditions, the unique contribution to the overall variance due to manipulations of T-2 could be estimated. Epochs of 6 s, beginning at the onset of the

T-1 cue, were used to model each pair; the 6-s epochs were convolved with a canonical hemodynamic response function. Correct and incorrect trials were modeled separately, and subsequent contrasts were restricted to correct trials. Effects were estimated by using a subject-specific fixed-effects model, with session-specific effects and low-frequency signal components treated as confounds. Linear contrasts were used to obtain subject-specific estimates for each effect. These estimates were entered into a second-level analysis treating subjects as a random effect, using a one-sample *t* test against a contrast value of zero at each voxel. Effects in the whole-brain analysis were considered reliable to the extent that they consisted of at least five contiguous voxels that exceeded an uncorrected threshold of $P < 0.001$. For the purpose of additional anatomical precision, group contrasts were also rendered on a Montreal Neurological Institute canonical brain that underwent cortical "inflation" using FREESURFER (CorTechs, Centreville, VA) (47, 48) and the SPM SURFEND toolbox (written by I. Kahn, Harvard University, Cambridge, MA).

The voxel-based contrasts were supplemented with ROI analyses to further characterize the effects of CSI and interference (RS vs. RD) in *a priori* expected regions, including mid-VLPFC. The ROI analyses were performed by using a toolbox for use with SPM99 (written by R. Poldrack, University of California, Los Angeles). ROIs included all significant (uncorrected $P < 0.001$) voxels within a 6-mm radius of the chosen maximum. Deconvolution allowed assessment of the signal change associated with each condition. ROI analyses were performed on measures of integrated percent signal change (peak ± 2 TRs) subjected to repeated-measures ANOVA. Finally, assessment of monotonic decay components over CSI in ROIs was performed by estimating a logarithmic decay in the switch vs. repeat difference for each subject individually and then entering these estimates into a second-level analysis that treated subject as a random variable, using a one-sample *t* test against a null effect value of 0. Decay in RT cost was assessed similarly, except that a linear rather than a logarithmic model was used, after residual analysis revealed that the distribution of errors deviated from normal. Likewise, convergence between the conflict output of the computational model and fMRI signal was evaluated within subject, based on a linear predictive relationship.

We thank R. Insler, I. Sturdivant, D. Pain, and S. Laszlo for assistance with data collection. This work was supported by the National Science Foundation (BCS 0401641), the Ellison Medical Foundation, the McKnight Endowment Fund for Neuroscience, and the Alfred P. Sloan Foundation.

- Jersild, A. T. (1927) *Arch. Psychol.*, no. 89.
- Allport, A. & Wylie, G. (2000) in *Control of Cognitive Processes: Attention and Performance*, eds. Monsell, S. & Driver, J. (MIT Press, Cambridge, MA), Vol. XVIII, pp. 35–70.
- Rubinstein, J. S., Meyer, D. E. & Evans, J. E. (2001) *J. Exp. Psychol. Hum. Percept. Perform.* **27**, 763–797.
- Monsell, S. (2003) *Trends Cognit. Sci.* **7**, 134–140.
- Logan, G. D. (2003) *J. Exp. Psychol. Hum. Percept. Perform.* **29**, 45–48.
- Rogers, R. D. & Monsell, S. (1995) *J. Exp. Psychol. Gen.* **124**, 207–231.
- Gilbert, S. J. & Shallice, T. (2002) *Cognit. Psychol.* **44**, 297–337.
- Yeung, N. & Monsell, S. (2003) *J. Exp. Psychol. Hum. Percept. Perform.* **29**, 919–936.
- Waszak, F., Hommel, B. & Allport, A. (2003) *Cognit. Psychol.* **46**, 361–413.
- Sohn, M.-H. & Anderson, J. R. (2003) *Mem. Cognit.* **31**, 775–780.
- Mayr, U. & Kliegl, R. (2000) *J. Exp. Psychol. Learn. Mem. Cognit.* **26**, 1124–1140.
- Petersen, S. E., Fox, P. T., Posner, M. I., Mintun, M. & Raichle, M. E. (1988) *Nature* **331**, 585–589.
- Thompson-Schill, S. L., D'Esposito, M., Aguirre, G. K. & Farah, M. J. (1997) *Proc. Natl. Acad. Sci. USA* **94**, 14792–14797.
- Badre, D., Poldrack, R. A., Paré-Blagoev, E. J., Insler, R. Z. & Wagner, A. D. (2005) *Neuron* **47**, 907–918.
- Badre, D. & Wagner, A. D. (2005) *Cereb. Cortex* **15**, 2003–2012.
- Jonides, J., Smith, E. E., Marshuetz, C., Koeppel, R. A. & Reuter-Lorenz, P. A. (1998) *Proc. Natl. Acad. Sci. USA* **95**, 8410–8413.
- Dobbins, I. G. & Wagner, A. D. (2005) *Cereb. Cortex* **15**, 1768–1778.
- Dove, A., Pollmann, S., Schubert, T., Wiggins, C. J. & von Cramon, D. Y. (2000) *Brain Res. Cognit. Brain Res.* **9**, 103–109.
- Brass, M. & von Cramon, D. Y. (2002) *Cereb. Cortex* **12**, 908–914.
- Brass, M. & von Cramon, D. Y. (2004) *J. Neurosci.* **24**, 8847–8852.
- Dreher, J.-C. & Grafman, J. (2003) *Cereb. Cortex* **13**, 329–339.
- Braver, T. S., Reynolds, J. R. & Donaldson, D. I. (2003) *Neuron* **39**, 713–726.
- Reynolds, J. R., Donaldson, D. I., Wagner, A. D. & Braver, T. S. (2004) *NeuroImage* **21**, 1472–1483.
- Rushworth, M. F., Hadland, K. A., Paus, T. & Sipila, P. K. (2002) *J. Neurophysiol.* **87**, 2577–2592.
- Crone, E. A., Wendelken, C., Donohue, S. E. & Bunge, S. A. (2006) *Cereb. Cortex* **16**, 475–486.
- Luks, T. L., Simpson, G. V., Feiwell, R. J. & Miller, W. L. (2002) *NeuroImage* **17**, 792–802.
- Sohn, M. H., Ursu, S., Anderson, J. R., Stenger, V. A. & Carter, C. S. (2000) *Proc. Natl. Acad. Sci. USA* **97**, 13448–13453.
- Allport, A., Styles, E. A. & Hsieh, S. (1994) in *Attention and Performance*, eds. Umiltà, C. & Moscovitch, M. (MIT Press, Cambridge, MA), Vol. XV, pp. 421–452.
- Meiran, N., Chorev, Z. & Sapir, A. (2000) *Cognit. Psychol.* **41**, 211–253.
- Cohen, J. D. & Servan-Schreiber, D. (1992) *Psychol. Rev.* **99**, 45–77.
- Ruge, H., Brass, M., Koch, I., Rubin, O., Meiran, N. & von Cramon, D. Y. (2005) *Neuropsychologia* **43**, 340–355.
- Botvinick, M. M., Braver, T. S., Barch, D. M., Carter, C. S. & Cohen, J. D. (2001) *Psychol. Rev.* **108**, 624–652.
- Hopfield, J. J. (1982) *Proc. Natl. Acad. Sci. USA* **79**, 2554–2558.
- Berlyne, D. E. (1957) *Psychol. Rev.* **64**, 329–339.
- Brass, M., Derrfuss, J., Forstmann, B. & von Cramon, D. Y. (2005) *Trends Cognit. Sci.* **9**, 314–316.
- Shadlen, M. N. & Newsome, W. T. (2001) *J. Neurophysiol.* **86**, 1916–1936.
- Bunge, S. A., Hazeltine, E., Scanlon, M. D., Rosen, A. C. & Gabrieli, J. D. (2002) *NeuroImage* **17**, 1562–1571.
- Schumacher, E. H. & D'Esposito, M. (2002) *Hum. Brain Mapp.* **17**, 193–201.
- Lorist, M. M., Klein, M., Nieuwenhuis, S., De Jong, R., Mulder, G. & Meijman, T. F. (2000) *Psychophysiology* **37**, 614–625.
- Rushworth, M. F., Passingham, R. E. & Nobre, A. C. (2002) *J. Cognit. Neurosci.* **14**, 1139–1150.
- Brass, M., Ullsperger, M., Knoesche, T. R., von Cramon, D. Y. & Phillips, N. A. (2005) *J. Cognit. Neurosci.* **17**, 1367–1375.
- Logan, G. D. & Bundesen, C. (2003) *J. Exp. Psychol. Hum. Percept. Perform.* **29**, 575–599.
- Rogers, R. D., Sahakian, B. J., Hodges, J. R., Polkey, C. E., Kennard, C. & Robbins, T. W. (1998) *Brain* **121**, 815–842.
- Rushworth, M. F., S., Hadland, K. A., Gaffan, D. & Passingham, R. E. (2003) *J. Cognit. Neurosci.* **15**, 338–353.
- Nelson, J. K., Reuter-Lorenz, P. A., Sylvester, C.-Y. C., Jonides, J. & Smith, E. E. (2003) *Proc. Natl. Acad. Sci. USA* **100**, 11171–11175.
- Coccosco, C. A., Kollokian, V., Kwan, R. K. S. & Evans, A. C. (1997) *NeuroImage* **5**, 425.
- Dale, A. M., Fischl, B. & Sereno, M. I. (1999) *NeuroImage* **9**, 179–194.
- Fischl, B., Sereno, M. I. & Dale, A. M. (1999) *NeuroImage* **9**, 195–207.